NEW METHOD FOR ESTIMATING THE DEPTH OF SMALL SURFACE-BREAKING CRACKS FROM PHOTO INDUCTIVE DATA

Ananth Sethuraman and James H. Rose
Center for Nondestructive Evaluation
Iowa State University
Ames, IA 50011

INTRODUCTION

Since the depth of surface-breaking cracks often determines the remaining life of a part, the characterization of surface-breaking cracks is a key problem in nondestructive evaluation. Eddy currents have been used for this purpose [1]. However, traditional eddy current methods have poor success when the dimensions of the crack are small compared with the inner radius of the eddy current probe. This is as expected, since the spatial resolution of an eddy current probe is comparable with its inner radius. Moulder *et al* [2] and Nakagawa [3] have described a new eddy-current based method of nondestructive evaluation, known as the photoinductive method. It offers greatly enhanced spatial resolution by combining the eddy current method with a laser. Images made with the photoinductive method provide a map of the surface-breaking portion of the crack and directly measure its length along the surface. In essence, the photoinductive method allows one to map the square, $\mathbf{E}\cdot\mathbf{E}$, of the electric field, $\mathbf{E}$, on the surface of the metallic part. In this paper, we develop and present a new method for estimating the depth and the shape of surface-breaking cracks in metallic parts from photoinductive data.

The remainder of this paper is arranged as follows. First, we state the problem. Next, we describe the principle of the photoinductive method. After this we turn to the work of Bowler [4], which offers the necessary mathematical physics. We pay particular attention to the eddy current half-space Green's function occurring in Bowler's work, as the rate of decay of the Green's function leads to what we term "the field of view", a concept useful in deciding the position of the laser focus points. Next, we present our method for estimating the crack depth and the crack shape from photoinductive measurements. We also present a simple example in which we tested the method. Finally we conclude with a brief summary.

PROBLEM STATEMENT

The test specimen is a metallic plate modeled as a half-space (Figure 1). Its top surface contains a line KL, which is the top edge of a surface-breaking crack, present in the test specimen. For simplicity, we suppose that the crack is tight and embedded in a vertical plane. Thus the crack may be modeled as a vertical, two-dimensional figure (Figure 1, hatched region KLM). The problem is to estimate the depth and the shape of this two-dimensional figure, using photoinductive measurements. To complete the description of the geometry, it should be pointed out that the laser employed in the photoinductive method can be focused only at a point on the top surface of the test specimen.

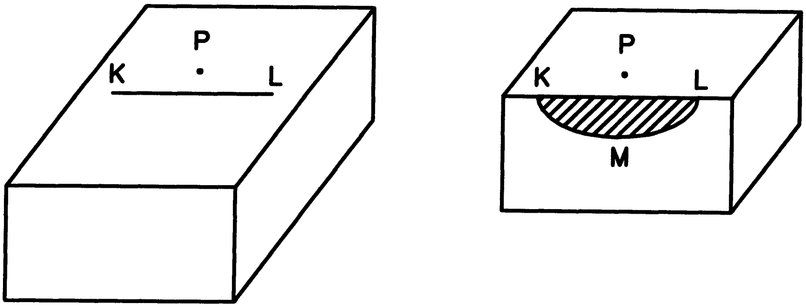

Figure 1. Left: A metallic part with a tight surface-breaking crack whose to edge is *KL*. *P* is a laser focus point. Right: A cut-away view of the metallic part showing the complete crack *KLM*.

THE PRINCIPLE OF THE PHOTOINDUCTIVE METHOD

As noted earlier, the photoinductive method combines eddy current inspection with a laser. The eddy current probe consists of a right-cylindrical air-core coil excited by an alternating current source and oriented with its axis normal to the surface to the surface of the test specimen. The laser is focused at a point P on the top surface of the test specimen and elevates the temperature in a region surrounding P (Figure 2, hatched region). The change in the temperature alters the conductivity of the metal at P and thus changes the impedance of the eddy current probe. Finally, $\mathbf{E}\cdot\mathbf{E}$, the (complex) square of the (complex) electric field, $\mathbf{E}$, at P can then be inferred from the change in the impedance.

Let I be current flowing through the eddy current probe, $\Delta\sigma$ the change in the conductivity due to the temperature rise, ΔZ the change in the impedance due to the temperature rise, $\Delta\mathbf{E}$ the change in the electric field, and V the volume of the heated region. An appeal to the reciprocity theorem [4-5] shows that

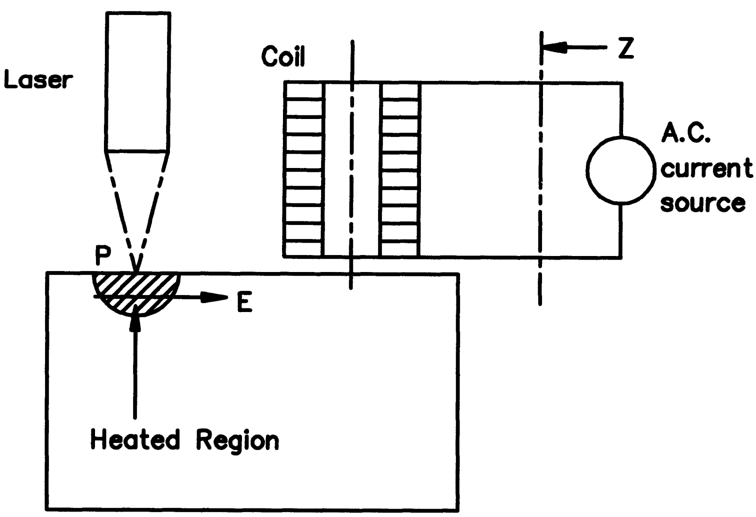

Figure 2. The apparatus of the photoinductive method. The change in the impedance ΔZ is proportional to the average of $\mathbf{E}\cdot\mathbf{E}$ in the heated region. The apparatus design makes the heated region small -- smaller than the inner radius of the coil. The figure is not to scale.

$$\Delta Z = \frac{-1}{I^2} \int_{heated\_region} \Delta\sigma(\mathbf{E} + \Delta\mathbf{E}) \cdot \mathbf{E} dV. \tag{1}$$

In addition, let ΔT denote the increase in the temperature, $d\sigma/dT$ the rate of change of the conductivity with respect to the temperature. Then if ΔT is small and the linear dimensions of the heated region are small, this formula can be simplified to

$$\Delta Z = \frac{-1}{I^2} \frac{d\sigma}{dT} \Delta T \mathbf{E} \cdot \mathbf{E} V. \tag{2}$$

The essence of this formula is that ΔZ is directly proportional to $\mathbf{E} \cdot \mathbf{E}$. We shall suppose that ΔZ can be measured with an impedance analyzer and that the constant of proportionality connecting ΔZ to $\mathbf{E} \cdot \mathbf{E}$ can be determined beforehand by an exercise of calibration. Then we shall have a method of measuring $\mathbf{E} \cdot \mathbf{E}$ at the point P. As the laser is movable, we can scan the top surface of the test specimen, *i.e.*, vary the laser focus point P to obtain $\mathbf{E} \cdot \mathbf{E}$ for any point on the top surface of the test specimen.

We shall complete this section by mentioning certain miscellaneous facts. First, the formula for ΔZ may be spoken of as a Born approximation because, in going from Equation 1 to Equation 2, the change in the electric field, $\Delta\mathbf{E}$, is neglected. Next, the laser is operated in a chopped manner, enabling ΔZ to be detected as the change in the impedance that is synchronous with the chopping frequency of the laser. Moreover, during the off-periods, the test specimen cools down, so that ΔT is small at the laser focus point -- a condition required to derive Equation 2. Another important condition is that the linear dimensions of the heated region should be small in comparison with the inner radius of the coil. It is this condition that is responsible for the enhanced spatial resolution of the photoinductive method. Some of the factors affecting the linear dimensions of the heated region are the chopping frequency of the laser, the beam diameter of the laser and the thermal conductivity of the metal. The design of the apparatus should take these factors into consideration and ensure that the linear dimensions of the heated region indeed satisfy the condition quoted above. Finally, KL, the length of the crack (Figure 1) is permitted to be small in comparison with the inner radius of the coil.

BOWLER'S FORMULA

The work of Bowler [6] shows that the electric field $\mathbf{E}$ is given by

$$\mathbf{E} = \mathbf{E}_{no\_crack} + \int_{crack\_face} \mathbf{G} p \mathbf{n} dS, \tag{3}$$

where $\mathbf{E}_{no\_crack}$ is the electric field in the absence of the crack, $\mathbf{G}$ is the (dyadic) half-space Green's function to the (vector) Helmholtz's equation, p is a concept known as the current dipole density and $\mathbf{n}$ is the unit vector normal to the crack. Formulas for $\mathbf{E}_{no\_crack}$ and for $\mathbf{G}$ have been given in the literature [6-8]. As to p, it is usually not known beforehand, but there is a fact that is useful in determining it. The support of p -- the set of points where p is non-zero -- is nothing but the crack. The crack is considered to be insulating material and so blocks the eddy current. This leads to the equation

$$\mathbf{E} \cdot \mathbf{n} = 0, \tag{4}$$

valid everywhere on the support of p. This equation, combined with Equation 3, helps to determine p.

THE NEED FOR AN ARRAY OF LASER FOCUS POINTS

Let $\mathbf{r}$ denote a laser focus point and $\mathbf{r}'$ denote a point in the cross-section containing the crack. Let us write the Green's function, $\mathbf{G}$, more elaborately as $\mathbf{G}(\mathbf{r},\mathbf{r}')$. If the absolute value of $\mathbf{G}(\mathbf{r},\mathbf{r}')$ is large then it means that the electric field -- and hence the photoinductive measurement at $\mathbf{r}$ -- is sensitive to the presence or absence of a crack at $\mathbf{r}'$. Now $\mathbf{G}$ contains the factors $\exp(ikr)$ and $1/r^3$, where

$$k = (1+i)\,/\,skin\_depth,$$
$$r = |\mathbf{r} - \mathbf{r}'|.$$

To study the consequences of this fact, let $P1$, $P2$ and $P3$ be laser focus points situated at different distances from the top edge of the crack KL. And let the cross-section containing the crack be divided into squares (Figure 4), with the squares marked 1, 2 or 3 being cracked. Then, remembering that the absolute value of $\mathbf{G}(\mathbf{r},\mathbf{r}')$ indicates the sensitivity to the presence of cracks, we find that photoinductive measurement at $P1$ is sensitive mainly to the presence or absence of cracks inside the square marked 1. We say that the field of view of $P1$ is the square marked 1. Similarly, the photoinductive measurement at $P2$ is sensitive mainly to the presence or absence of cracks inside the squares marked 1 and 2. We say that the field of view of $P2$ comprises the squares marked 1 or 2. Similarly, the field of view of $P3$ comprises the squares marked 1, 2 or 3. The field of view will be helpful in the procedure of estimating the crack depth and the crack shape, a procedure that we shall speak of as inversion.

INVERSION METHOD

Let the cross-section containing the crack be divided into squares of size a. W divide the squares into three categories:

(i) squares known beforehand to be intact;
(ii) squares known beforehand to be cracked; and
(iii) unknown squares, i.e., it is not known beforehand whether these squares are cracked or intact.

The current dipole density p is assumed to be uniform in each square, and a guess is made for its values according to the following rules:

(i) For each square known beforehand to be intact, put $p = 0$.

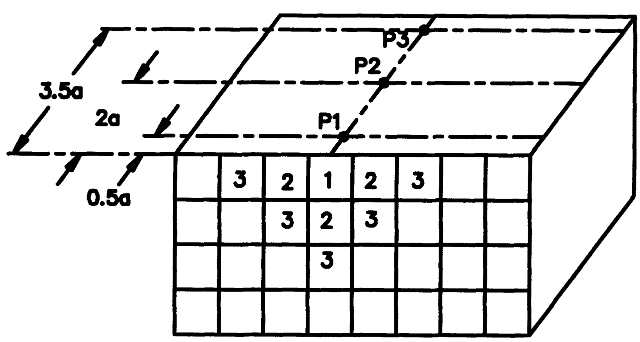

Figure 3. $P1$, $P2$ and $P3$ are different laser focus points. $P1$'s field of view is the square marked 1. $P2$'s field of view comprises the squares marked 1 and 2. $P3$'s field of view comprises the squares marked 1, 2 and 3.

(ii) For each square known beforehand to be cracked, make a guess of p . A useful heuristic rule, valid when the skin depth is somewhat greater than the number of rows of squares $\times\ a$, is that the guess should be in the neighborhood of $\sigma \mathbf{E} \cdot \mathbf{n}\, a$.
(iii) For each unknown square, guess whether it is intact or cracked, and, accordingly, use the rules stated above.

The correctness of these guesses is verified as follows:
(i) Substitute the guess for p in Bowler's formula and compute $\mathbf{E}$ at the centers of all the squares, and at the laser focus points.
(ii) For each square known beforehand to be cracked, check that $\mathbf{E} \cdot \mathbf{n} = 0$, or equivalently, that

$$\sum |\mathrm{E}\ \mathbf{n}|^2 = 0, \tag{5}$$

the sum being computed over all squares known beforehand to be cracked.
(iii) Each unknown square is either intact, in which case $p = 0$; or cracked, in which case
$\mathbf{E} \cdot \mathbf{n} = 0$. In either case, check that $p\ \mathbf{E} \cdot \mathbf{n} = 0$, or equivalently, that

$$\sum |p\mathrm{E}\ \mathbf{n}|^2 = 0, \tag{6}$$

the sum being computed over all unknown squares.
(iv) For each laser focus point, check that the computed value of $\mathbf{E} \cdot \mathbf{E}$ agrees with the measured value, or equivalently, that

$$\sum |(\mathbf{E} \cdot \mathbf{E})_{measured} - (\mathbf{E} \cdot \mathbf{E})_{calculated}|^2 = 0, \tag{7}$$

the sum being computed over all laser focus points.

If the guesses meet these checks, they are accepted as being correct. The crack is then estimated as being the set of all squares whose current dipole density p is non-zero. If the guesses fail to meet one or more of these checks, new guesses must be generated and the checks performed on them.

Let use consider Equations 5-7. Let F denote the sum of the left hand sides of these equations. Then the steps described above have the effect of minimizing F. The entire exercise amounts to one of minimization, with F as the objective function, and the current dipole densities of the squares as the unknowns. The minimization can be done with a standard minimization algorithm, *e.g.*, the Monte Carlo algorithm.

ILLUSTRATING THE INVERSION METHOD WITH SYNTHETIC DATA

We tested the proposed inverse method with synthetic data for a series of cracks with an aspect ratio of 2:1 in titanium and aluminum, as shown in Figure 4. Note that titanium has a low conductivity and aluminum has a high conductivity. Cracks of two sizes were chosen: either a length of 400 μm and a depth of 200 μm; or a length of 200 μm and a depth of 100 μm. We describe below the inversion procedure for these test cases.

We began by dividing the cross-section containing the crack into squares of size a (100 μm for the larger cracks and 50 μm for the smaller cracks). We chose the eddy current angular frequency ω such that the skin depth was slightly greater than $0.5a$. Next, we chose a single laser focus point, the point situated $0.5a$ from the top edge of the crack (Figure 5). Only the square marked (1,1) was in the field of view of this laser focus point, and the inversion method was able to estimate only its current dipole density. For all the test

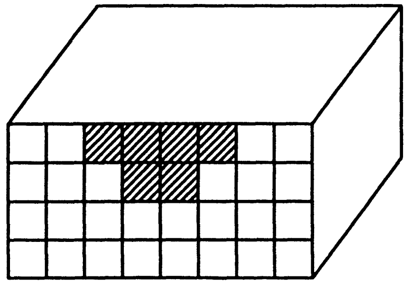

Figure 4. The actual shape of the crack. The hatched squares are cracked, the others intact. The forward problem was carried out on this crack to generate synthetic data.

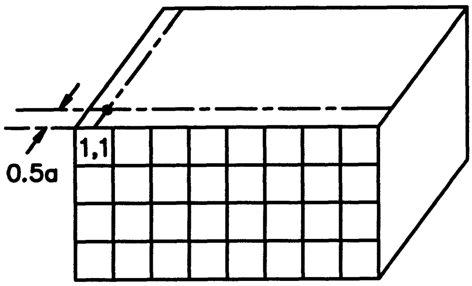

Figure 5. The laser focus point has the square marked 1,1 in its field of view. Synthetic data generate for this laser focus point helps to estimate the condition, whether intact or cracked, of the square marked 1,1.

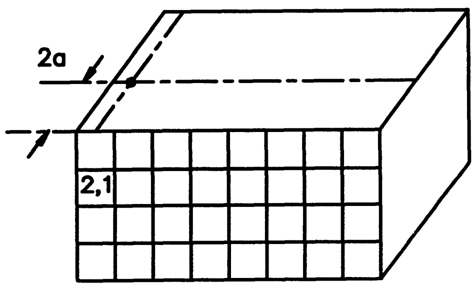

Figure 6. The laser focus point has the square marked 2,1 in its field of view. Synthetic data generate for this laser focus point helps to estimate the condition, whether intact or cracked, of the square marked 2,1.

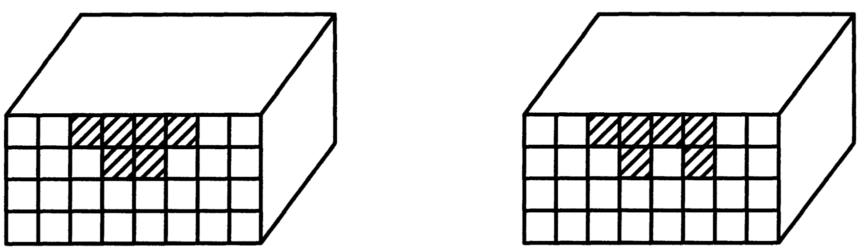

Figure 7. Two cracks that give rise to nearly the same photoinductive data. The instability of the algorithm with respect to noise and the Monte Carlo seed is nothing but a sign that more than one crack gives rise to nearly the same photoinductive data.

cases considered, the method estimated that the current density of the square marked (1,1) was zero and thus that this square was intact. Next, we shifted the laser focus point and the eddy current probe to the right by a distance a. The whole exercise was repeated and it was found that the square marked (1,2) was also intact for all the cracks considered. The procedure accurately determined the condition, whether intact or cracked, of all the squares in the first row.

Next, we determined the condition of the squares in the second layer, supposing that the condition of the first layer had been accurately determined. We chose the laser focus point to be one situated about $2a$ from the top edge of the crack (Figure 6) and chose the skin depth to be somewhat greater than $2a$. Now the square marked (2,1) was in the field of view, and the inversion method accurately determined this square to be intact. By shifting the laser focus point and the coil to the right in steps of a, we estimated the condition, whether intact or cracked, of each square in the second row. The method accurately determined the condition of the squares in the second row. In this way, we were able to accurately determine the size and the shape of the crack in each test case. But we must qualify this remark with an observation about ill-posedness.

As suggested previously, our computer program operated by using a Monte Carlo algorithm to minimize F . Therefore one of the inputs was a negative integer -- the "seed" -- to start the generation of a sequence of pseudo-random numbers. It was necessary to check that the results of the computer program were the same, no matter what the seed. In one case, we found that the predictions for two adjacent squares in the second row were exchanged on changing the seed (Figure 7). On running the forward problem to the two cracks depicted in Figure 7, we found that the values of $\mathbf{E} \cdot \mathbf{E}$ were nearly the same. This showed that the problem was inherently ill-posed. The ill-posedness was not noticed in the first row of squares, and only in one case in the second row of squares. When we considered three rows of squares, the ill-posedness became more frequent. The addition of a small quantity of noise to $\mathbf{E} \cdot \mathbf{E}$ also gave rise to the same kind of ill-posedness.

SUMMARY

We have proposed a method for determining the *depth* of surface breaking cracks from photoinductive images. We introduced the concept of the "field of view", which leads to a systematic procedure for determining the laser focus points. Finally, we tested the proposed method by estimating the depth of small cracks in titanium and aluminum from synthetic data.

ACKNOWLEDGMENTS

This work was supported by the NSF Industry / University Center for Nondestructive Evaluation at Iowa State University. We thank Norio Nakagawa for making his boundary element program for the forward problem available for our use and John Moulder for discussions of various aspects of the experimental problem.

REFERENCES

1. J.R.Bowler, S.J.Norton and D.J.Harrison, Eddy current interaction with an ideal crack Part I: The inverse problem, Journal of Applied Physics 75(12):8134-8144 (1994).
2. J.C.Moulder, N.Nakagawa, K.S.No, Y.P.Lee and J.F.McClelland, Photoinductive imaging: a new NDE technique, In D.O.Thomson and D.E.Chimenti, editors, Review of Progress in Quantitative Nondestructive Evaluation, Volume 8A, pages 599-606, Plenum (1989)

3. N.Nakagawa, Theory of eddy current inspection of corner cracks, In D.O.Thomson and D.E.Chimenti, editors, Review of Progress in Quantitative Nondestructive Evaluation, Volume 10A, pages 249-254, Plenum (1991)
4. B.A.Auld, Theoretical characterization and comparison of resonant-probe microwave eddy-current testing with conventional low--frequency eddy-current methods, In G.Birnbaum and G.Free, editors, Eddy-Current Characterization of Materials and Structures, ASTM STP 722, pages 332-347 (1981)
5. R.Satveli, Software modeling for flaw characterization of metals through eddy-currents, M.S.Thesis, Iowa State University, pages 22-28 (1995)
6. J.R.Bowler, Eddy current interaction with an ideal crack Part I: the forward problem, Journal of Applied Physics, 75(12):8128-8137 (1994)
7. C.V.Dodd and W.E.Deeds, Analytical solutions to eddy-current probe-coil problems, Journal of Applied Physics 6(6):2829-2835 (1968)
8. A.P.Raiche and J.H.Coggon, Analytic Green's tensors for integral equation modeling, The Geophysical Journal of the Royal Astronomical Society, 42:1035-1038 (1975)